

Size-dependent mechanical properties of molybdenum nanopillars

Ju-Young Kim^{a)} and Julia R. Greer

Division of Engineering and Applied Science, California Institute of Technology,
Pasadena, California 91125, USA

(Received 1 July 2008; accepted 16 August 2008; published online 12 September 2008)

We report the deformation behavior of single crystalline molybdenum nanopillars in uniaxial compression, which exhibits a strong size effect called the “smaller is stronger” phenomenon. We show that higher strengths arise from the increase in the yield strength rather than through postyield strain hardening. We find the yield strength at nanoscale to depend strongly on sample size and not on the initial dislocation density, a finding strikingly different from that of the bulk metal. © 2008 American Institute of Physics. [DOI: 10.1063/1.2979684]

Efforts to characterize the mechanical deformation behavior of materials at nanoscale have been driven by the need for precise fabrication and reliable operation of nanoscale devices as well as by fundamental scientific curiosity.^{1–16} Uniaxial compression tests of micropillars and nanopillars, recently used to investigate size-dependent mechanical properties at this scale, have shown that pure metals and metallic alloys exhibit strong size effects in plastic deformation, called the “smaller is stronger” phenomenon.^{2–10} As metal sample sizes decrease to nanoscale, they are expected to contain few or no dislocations, and dislocations generated during plastic deformation tend to escape the crystal by annihilating at a nearby free surface, a condition known as hardening by dislocation starvation.^{3–5,7–10} However, other origins of size effects in plastic deformation of nanocrystals remain somewhat controversial.

Here we report the size dependence of mechanical behavior of single-crystal molybdenum (Mo) [body-centered cubic (bcc)] nanopillars. The uniaxial stress-strain curves of these nanopillars appear to have the following two distinct features not present in previous experimental reports for Ni, Ni₃Al, and Au [face-centered cubic (fcc)]:^{2–4,7,8} (1) onset of plasticity is unambiguous allowing for precise yield strength determination, and (2) plastic deformation region is composed of discrete strain bursts (believed to be associated with dislocation annihilation) and continuous strain hardening (associated with dislocation multiplication), which may lead to the overall increase in dislocation density during plastic deformation. In this study, smaller Mo nanopillars are found to sustain higher stress even though they do not meet the condition of dislocation starvation. We show that the fundamental origin of the observed size effect (higher strength for smaller sample) is the pronounced increase in yield strength, which is found to strongly depend on the pillar size and, surprisingly, to be independent of the initial dislocation density.

Nanopillars with diameters from ~200 to ~900 nm and aspect ratios (height/diameter) of ~3 were made from electropolished and well annealed (100) single-crystal Mo using the focused ion beam (FIB) (Nova 200 NanoLab, FEI Co., Hillsboro, OR, USA) fabrication technique.^{2,3} The nanopillars were subsequently compressed by a Nanoindenter G200 (Agilent Corp., Oak Ridge, TN, USA) with a flat punch tip of 30 μm diameter at a constant nominal displacement rate

of 2 nm/s. In order to investigate the effects of surfaces on strength, nanoannuli, or cylinders with through holes in their center, with the outer diameter of ~1000 nm, the inner hole diameter of ~500 nm, and the height of ~2000 nm were also micromachined by FIB and then compressed. To assess the impact of the initial dislocation density, nanopillars with high initial dislocation density (HIDD) were micromachined in the severely deformed plastic zone of the residual nanoindentation marks, which were formed at 800 nm maximum indentation depth using a three-sided Berkovich indenter, and then compressed.

Figure 1(a) shows several typical true stress-true strain curves with some intentional unloading-and-reloading segments. Yield strengths were determined based on these plots as the first strain burst for nanopillars of diameter greater than ~600 nm and by the 0.2% offset method for the smaller nanopillars since they did not exhibit such a clear initiation of plastic flow. These yield points clearly identify the transition from the initial linear elastic to plastic deformation through nonlinear strain hardening. Figure 1(a) shows the yield strengths and flow stresses attained at ~7% true strain as a function of nanopillar diameter (on log-log scale). The lack of ambiguity in the yield point may be caused by the relatively high strength of Mo (above ~400 MPa), slow axial displacement rate (2 nm/s), and improved data acquisition rate (25 Hz) over previously reported experiments. Some data points in Fig. 1(b) have been reported in the work of Brinckmann *et al.*⁹ The HIDD nanopillars are subsequently discussed. Figures 1(a) and 1(b) clearly show that substantially higher flow stresses and yield strengths are attained with decreasing nanopillar size. However, the slopes of yield strength and flow stress curves versus pillar diameter on log-log scale are -0.44 and -1.07,

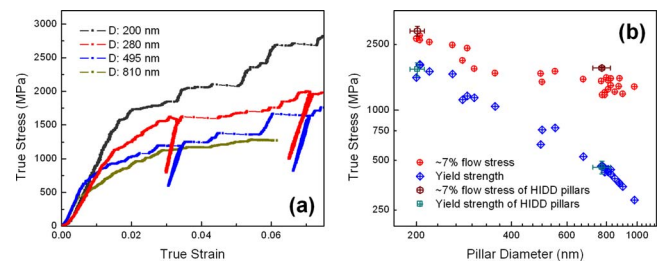


FIG. 1. (Color online) Size-dependent deformation behavior of Mo nanopillars in uniaxial compression: (a) Typical stress-strain curves. (b) Flow stress at ~7% true strain and yield strength vs pillar diameter, showing strong size effects.

^{a)}Electronic mail: jyk@caltech.edu.

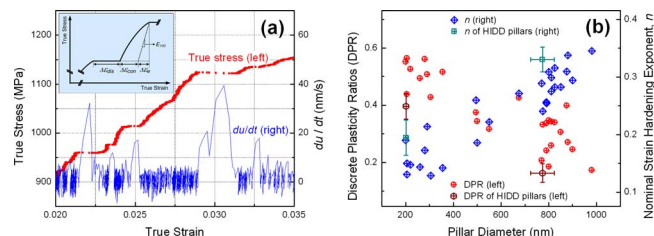


FIG. 2. (Color online) Contribution of discrete strain bursts and overall strain hardening in plastic deformation. (a) Overlap of stress-strain curve and axial displacement rate du/dt for the pillar of diameter 790 nm. (b) Discrete plasticity ratios (DPR) and nominal strain-hardening exponent, n , which show the decrease in contribution of discrete strain burst and strain hardening as the pillar size decreases.

respectively, which indicates that the size effect in yield strength is much more pronounced than that in flow stress.

To evaluate the contributions of discrete and continuous deformation segments to the overall plastic strain, we employ the discrete plasticity ratio.¹⁷ A typical stress-strain curve in the plastic region consists of the following three distinct parts: discrete strain burst ($\Delta\epsilon_{dis}$), continuous strain hardening ($\Delta\epsilon_{con}$), and elastic region ($\Delta\epsilon_e$), which is recovered during unloading [see inset in Fig. 2(a)]. We utilize the ratio of the sum of discrete portions and the total plastic strain, $[\sum\Delta\epsilon_{dis,i}/(\sum\Delta\epsilon_{dis,i}+\sum\Delta\epsilon_{con,i})]$, as a measure of the contribution of discrete events to the overall plastic strain. We identify an event as a discrete burst when the axial displacement rate (du/dt) is greater than 10 nm/s.⁹ Figure 2(a) shows that using this methodology, a strain burst can be clearly identified. If a $\{110\}/\langle 111 \rangle$ crystallographic slip sys-

tem is assumed to be operating during uniaxial compression of $\langle 001 \rangle$ -oriented bcc Mo, one slip event corresponds to a $\langle 100 \rangle$ axial displacement of 0.157 nm ($|\vec{b}|/\sqrt{3}$, where \vec{b} is the Burgers vector). Since this value is below the sensitivity of the existing nanoindentation equipment, strain bursts below the estimated criterion inevitably include the plastic portion of the continuous strain hardening. We find that the discrete plasticity ratio increases with decreasing pillar size, as shown in Fig. 2(b). We believe this may be caused by the easier annihilation of some dislocations at the surface in the smaller pillars.

To evaluate the extent of overall strain hardening during plastic deformation, the nominal strain hardening exponent n is estimated as calculated from the slope between yield point and 7% flow stress point in log-log plot. The n is found to decrease with pillar size, as shown in Fig. 2(b), which means that the contribution of strain hardening during deformation decreases with pillar size. These findings indicate that the main mechanism for the higher flow stress in the smaller pillars is not postyield strain hardening but a strong yield strength dependence on size.

Unlike in previously reported fcc Ni, Ni₃Al, and Au,²⁻⁴ the combination of elastic loadings followed by discrete strain bursts is not dominant even in the smallest Mo pillars ($\sim 200 \text{ nm}$ diameter). Here, the nonlinear strain hardening remains a significant part of the curve, which most likely means that dislocation density is evolving via the creation and functioning of Frank-Read sources, which continuously supply newly generated dislocations throughout the deforma-

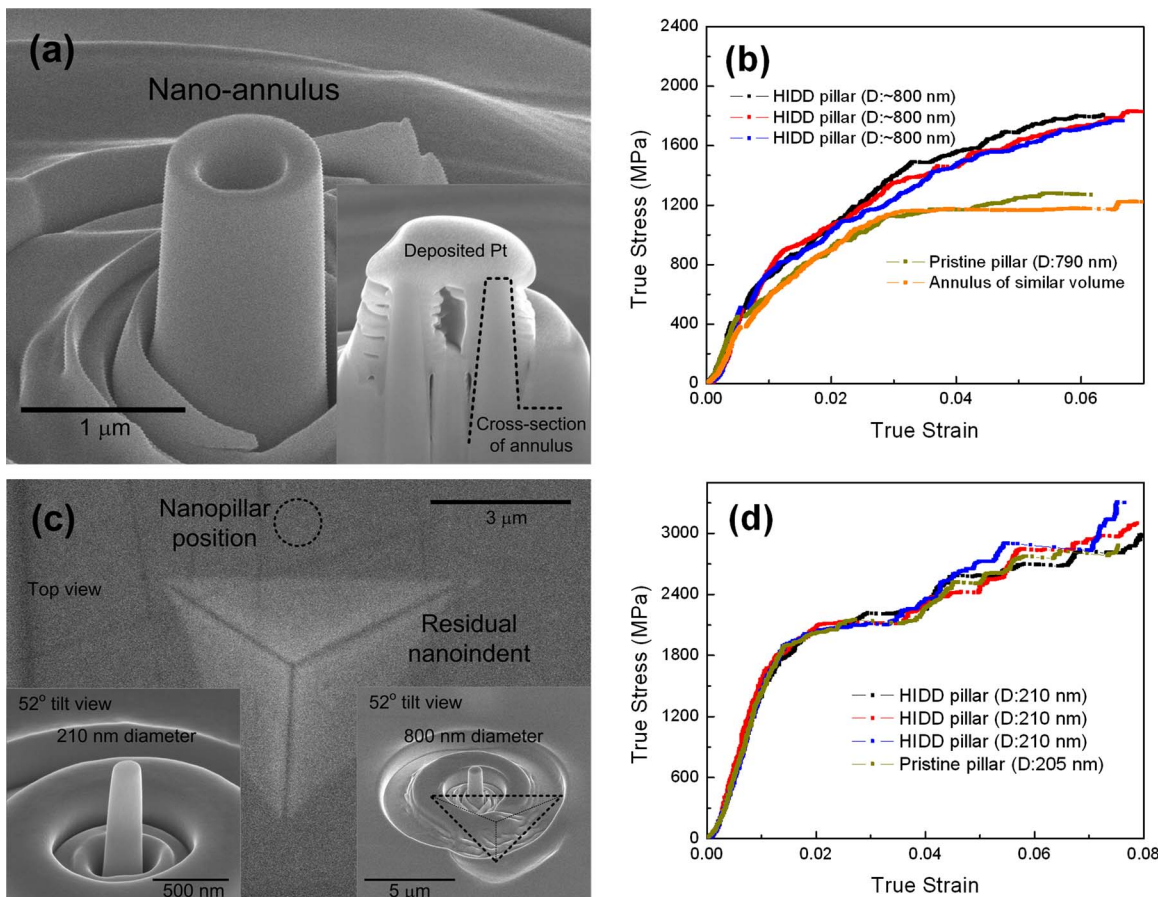


FIG. 3. (Color online) Stress-strain behaviors of annuli with higher surface-to-volume ratio and nanopillars of HIDD micromachined near residual nanoindentations.

tion. Although the escape of dislocations at the surface becomes possible as the nanopillar size decreases, the continuous supply of dislocations by dislocation multiplication prevents the condition of total dislocation starvation in these pillars, thus only reducing rather than eliminating the strain hardening behavior.^{9,10}

This observed size effect on yield strength might be due to the oxide surface layer¹⁸ or a hardened surface layer introduced during FIB milling.¹⁹ To determine the effects of relative surface area on the size effect, we fabricated several annuli with ~ 1000 nm outer diameter, ~ 500 nm inner hole diameter, and ~ 2000 nm height by using FIB, as shown in Fig. 3(a). The deformed volume of the annulus is similar to that of the ~ 800 nm diameter nanopillar ($\sim 1.2 \text{ nm}^3$), while the surface area of the annulus is ~ 1.6 times greater than that of the nanopillar. A typical annulus stress-strain curve is presented in Fig. 3(b). The yield point is clearly measurable by the first strain burst. If the hardened surface layer contributed significantly to the strength of the specimen, the yield strengths of the annuli would be expected to be higher than those of the similar-volume pillars. However, the yield strengths of the annuli appear to be $400.7 (\pm 31.6)$ MPa (measured from four annuli), nearly identical with those of the similar-volume pillars. This result implies that the increase in yield strength is most likely not caused by the presence of a hardened surface, and that incipient plasticity is most probably caused by dislocation activity in the bulk of the pillar as well as at the free surface.

To examine the effects of initial dislocation density on plasticity of nanocrystal, several nanopillars with diameters of ~ 200 and ~ 800 nm were micromachined near residual nanoindentations, as shown in Fig. 3(c). They are referred to as HIDD pillars. The dislocation density of the pristine material was evaluated as $3.4 \times 10^9 (\pm 1.7 \times 10^9) \text{ m}^{-2}$ by the etch-pits technique.²⁰ The dislocation density in the plastic zone around the residual nanoindentations was estimated from the measured indentation hardness (2.38 ± 0.01 GPa) and the Nix-Gao model¹² as $7.5 \times 10^{14} \text{ m}^{-2}$, implying that nanopillars fabricated from this region are expected to have initial dislocation densities five orders of magnitude greater than the pristine nanopillars. The stress-strain curves of HIDD pillars are shown in Figs. 3(b) and 3(d), and the evaluated yield strengths, flow stresses, discrete plasticity ratios, as well as the nominal strain hardening exponents are shown in Figs. 1(b) and 2(b). It is clear that the yield strength of HIDD pillars is very similar to that of the pristine ones, and the 7% flow stress is slightly higher, as shown in Fig. 1(b). The discrete plasticity ratio is slightly lower, and the nominal strain hardening exponent is slightly higher, as shown in Fig. 2(b). These results strongly suggest that higher initial dislocation density does not significantly affect the yield strength at nanoscale regardless of sample size. Strain hardening, however, is more pronounced in the HIDD nanopillars. In the course of plastic deformation of the nanopillar, as mentioned

above, there is an added contribution of dislocation density decrease via annihilation at the free surface. The observed high rate of strain hardening in the HIDD nanopillars is most likely due to the high initial density of the existing dislocations impeding the motion of the gliding dislocations during deformation, which causes the overall increase in dislocation density. Our findings imply that the yield phenomenon at nanoscale strongly depends on the sample size and not on the initial dislocation density, which are consistent with the similar observed yield strengths of Ni nanopillars, whose initial dislocation density was $\sim 10^{15} \text{ m}^{-2}$, and which were made dislocation-free by mechanical annealing.⁸

In summary, our work reveals that the higher flow stresses attained by the smaller Mo pillars are attributed more to the pronounced increase in yield strength rather than to any other mechanism. We showed that the size effect in yield strength is not likely to be caused by surface hardening due to the presence of an oxide layer or created as a result of FIB milling, and cannot be explained with conventional Taylor hardening model. Instead, it is consistent with the lower probability of finding atoms to initiate plasticity in smaller samples, thereby requiring the application of higher stresses. Hardening by dislocation starvation prevalent in fcc materials is not found here, which might be because the dislocations continue to be generated even in the smallest Mo (bcc) pillars.

¹S. S. Brenner, *J. Appl. Phys.* **27**, 1484 (1956).

²M. D. Uchic, D. M. Dimiduk, J. N. Florando, and W. D. Nix, *Science* **305**, 986 (2004).

³J. R. Greer, W. C. Oliver, and W. D. Nix, *Acta Mater.* **53**, 1821 (2005).

⁴J. R. Greer and W. D. Nix, *Phys. Rev. B* **73**, 245410 (2006).

⁵W. D. Nix, J. R. Greer, G. Feng, and E. T. Lilleodden, *Thin Solid Films* **515**, 3152 (2007).

⁶D. M. Dimiduk, C. Woodward, R. LeSar, and M. D. Uchic, *Science* **312**, 1188 (2006).

⁷C. A. Volkert and E. T. Lilleodden, *Philos. Mag.* **86**, 5567 (2006).

⁸Z. W. Shan, R. K. Mishra, S. A. Syed Asif, O. L. Warren, and A. M. Minor, *Nat. Mater.* **7**, 115 (2008).

⁹S. Brinckmann, J.-Y. Kim, and J. R. Greer, *Phys. Rev. Lett.* **100**, 155502 (2008).

¹⁰J. R. Greer, C. R. Weinberger, and W. Cai, *Mater. Sci. Eng., A* **493**, 21 (2008)

¹¹H. Bei, S. Shim, E. P. George, M. K. Miller, E. G. Herbert, and G. M. Pharr, *Scr. Mater.* **57**, 397 (2007).

¹²W. D. Nix and H. J. Gao, *J. Mech. Phys. Solids* **46**, 411 (1998).

¹³J.-Y. Kim, B.-W. Lee, D. T. Read, and D. Kwon, *Scr. Mater.* **52**, 353 (2005).

¹⁴J.-Y. Kim, S.-K. Kang, J.-J. Lee, J.-i. Jang, Y.-H. Lee, and D. Kwon, *Acta Mater.* **55**, 3555 (2007).

¹⁵J.-Y. Kim, S.-K. Kang, J. R. Greer, and D. Kwon, *Acta Mater.* **56**, 3338 (2008).

¹⁶E. Rabkin, H.-S. Nam, and D. J. Srolovitz, *Acta Mater.* **55**, 2085 (2007).

¹⁷J.-i. Jang, B.-G. Yoo, and J.-Y. Kim, *Appl. Phys. Lett.* **90**, 211906 (2007).

¹⁸J. J. Gilman, *Science* **306**, 1134 (2004).

¹⁹H. Bei, S. Shim, M. K. Miller, G. M. Pharr, and E. P. George, *Appl. Phys. Lett.* **91**, 111915 (2007).

²⁰H. L. Prekel and A. Lawley, *Philos. Mag.* **14**, 545 (1966).